HHS Public Access

Author manuscript

Environ Sci Technol. Author manuscript; available in PMC 2018 October 19.

Published in final edited form as:

Environ Sci Technol. 2018 May 01; 52(9): 5469–5478. doi:10.1021/acs.est.8b00512.

Organohalogens Naturally Biosynthesized in Marine Environments and Produced as Disinfection Byproducts Alter Sarco/Endoplasmic Reticulum Ca^{2+} Dynamics

Jing Zheng[†,‡], **Shaun M. K. McKinnie**[§], **Abrahim El Gamal**[§], **Wei Feng**[†], **Yao Dong**[†], **Vinayak Agarwal**[#], **William Fenical**[#], **Abdhesh Kumar**[§], **Zhengyu Cao**[†,‡], **Bradley S. Moore**[§], and **Isaac N. Pessah**[*,†]

[†]Department of Molecular Biosciences, School of Veterinary Medicine, University of California, Davis, California 95616, United States

[‡]Department of TCM Pharmacology, School of Traditional Chinese Medicines, China Pharmaceutical University, Nanjing 210009, China

[§]Center for Oceans and Human Health, Scripps Institution of Oceanography & Skaggs School of Pharmacy and Pharmaceutical Sciences, University of California, San Diego, La Jolla, California 92093-0021, United States

Abstract

Contemporary sources of organohalogens produced as disinfection byproducts (DBPs) are receiving considerable attention as emerging pollutants because of their abundance, persistence, and potential to structurally mimic natural organohalogens produced by bacteria that serve signaling or toxicological functions in marine environments. Here, we tested 34 organohalogens from anthropogenic and marine sources to identify compounds active toward ryanodine receptor (RyR1), known toxicological targets of non-dioxinlike polychlorinated biphenyls (PCBs) and polybrominated diphenyl ethers (PBDEs). [^{3}H]Ryanodine ([^{3}H]Ry) binding screening (≤2 μM) identified 10 highly active organohalogens. Further analysis indicated that 2,3-dibromoindole (**14**), tetrabromopyrrole (**31**), and 2,3,5-tribromopyrrole (**34**) at 10 μM were the most efficacious at enhancing [^{3}H]Ry binding. Interestingly, these congeners also inhibited microsomal sarcoplasmic/endoplasmic reticulum (SR/ER) Ca^{2+} ATPase (SERCA1a). Dual SERCA1a inhibition and RyR1 activation triggered Ca^{2+} efflux from microsomal vesicles with initial rates rank ordered **31** > **34** > **14**. Hexabromobipyrroles (**25**) enhanced [^{3}H]Ry binding moderately with strong SERCA1a inhibition, whereas pyrrole (**24**), 2,3,4-tribromopyrrole (**26**), and ethyl-4-bromopyrrole-2-carboxylate (**27**) were inactive. Of three PBDE derivatives of marine origin active in the [^{3}H]Ry assay, 4′-hydroxy-2,3′,4,5′,6-pentabromodiphenyl ether (**18**) was also a highly potent SERCA1a

[*]**Corresponding Author** inpessah@ucdavis.edu. Telephone: +1-(530)-7526696.

[#]**Present Address** Parker H. Petit Institute for Bioengineering & Bioscience, Georgia Institute of Technology, Atlanta, Georgia 30332, United States.

The authors declare no competing financial interest.

Supporting Information

The Supporting Information is available free of charge on the ACS Publications website at DOI: 10.1021/acs.est.8b00512.

Detailed materials and methods, synthetic procedures, and supplemental results (PDF)

inhibitor. Molecular targets of marine organohalogens that are also DBPs of emerging environmental concern are likely to contribute to their toxicity.

GRAPHICAL ABSTRACT

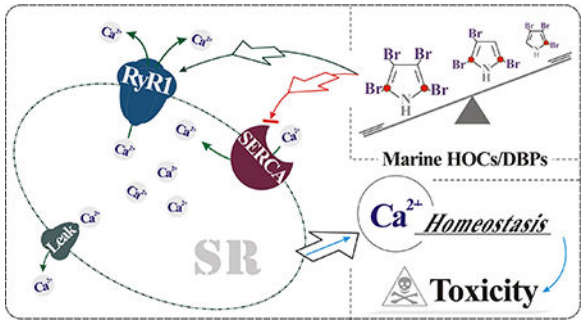

INTRODUCTION

Halogenated organic compounds (HOCs) are pervasive in natural and built environments.[1–10] Despite restrictions and banning in most parts of the world through the Stockholm Convention on Persistent Organic Pollutants (POPs), levels of well-studied “legacy” compounds, including polychlorinated biphenyls (PCBs) and polybrominated diphenyl ethers (PBDEs), are routinely detected in human and wildlife tissues where they continue to pose significant health risks to highly exposed and susceptible populations.[11–17] In addition to anthropogenic sources, more than 4,500 HOCs are synthesized by microbes and algae,[1,18] and many of these natural products strongly resemble banned anthropogenic chemicals or their metabolites. For example, marine bacteria express enzymes that synthesize OH-PBDEs and their derivatives.[1,19–22] Like their anthropogenic counterparts, marine HOCs accumulate in marine mammals, Antarctic air, seabird eggs, and human breast milk, possibly adding to adverse health risks.[23–27] Recently, the biosynthetic pathways for a number of brominated pyrroles, bipyrroles and phenols have been also elucidated.[1,19,21,28] Tetrabromopyrrole (**31**) isolated from Pseudoalteromonas bacteria has been shown to elicit specific development cues to coral larvae necessary for metamorphosis and benthic attachment of *Orbicella franksi and Acropora palmata* onto crustose coralline algae.[29,30] Remarkably, high levels of several halopyrroles, including tetrabromopyrrole (**31**), are produced as disinfection byproducts (DBPs) during treatment of drinking water, agricultural irrigation water and saline wastewater, and are considered as emerging pollutants because of their cytotoxicity, genotoxicity, carcinogenicity and developmental toxicity.[31–35] For example, **31** is a prominent byproduct of chlorination of seawater for sewage-treatment in coastal areas and exhibits potent developmental toxicity to *Platynereis dumerilii* embryos.[34] Another DBP first identified in Israeli drinking water, 2,3,5-tribromopyrrole (**34**), is produced during sewage treatment protocols utilizing both chlorine and seawater that are common in coastal communities, and is genotoxic and cytotoxic to CHO (Chinese hamster ovary) cells.[31,32]

Legacy HOCs are known to disrupt a number of biological processes that mediate toxicological sequelae across life stages. Two well studied direct molecular targets include (1) the aryl hydrocarbon hydroxylase receptor (AhR) modulated by coplanar dioxin-like

HOCs that alter expression of AhR responsive genes and (2) ryanodine receptors (RyRs), anchored within sarcoplasmic/endoplasmic (SR/ER) membranes of most invertebrate and vertebrate cell types, which bind noncoplanar (nondioxin-like; NDL) HOCs and alter Ca^{2+} homeostasis. RyRs, along with genetically related inositol-1,3,5trisphosphate receptors (IP_3R) affect the release of Ca^{2+} from SR/ER stores in response to physiological, pharmacological and environmental cues, and thus are critical components mediating a myriad of Ca^{2+}-regulated cellular processes.[16,36,37] Ca^{2+} release into the cytoplasm is countered by highly active energy-dependent reaccumulation of Ca^{2+} into the microsomal lumen by the SR/ER Ca^{2+}-ATPase (SERCA) pumps.

We observed that many of the natural HOCs identified to date are NDL structures that would be predicted to have activity toward RyRs and could disrupt Ca^{2+} dynamics and Ca^{2+}-dependent signaling pathways.[16] Experiments were performed to define the structure −activity relationship of 34 HOCs using [^{3}H]Ry binding analysis. Ten natural/anthropogenic halogenated pyrroles, maleimides, bipyrroles, indoles, and diphenyl ether are identified as potent direct modulators of RyR1. Moreover, several of these RyR-active HOCs are also potent SERCA1a inhibitors. These two molecular actions result in rapid Ca^{2+} efflux from microsomal vesicles consistent with the opposing influences of RyR1 and SERCA1a on SR/ER Ca^{2+} balance. These results are the first to identify molecular targets of marine organohalogens that are also DBPs of emerging environmental concern and are likely to contribute to their cellular neurotoxicity reported (unpublished work).

■ MATERIALS AND METHODS

Chemicals and Reagents.

Organohalogens were custom synthesized as described in the Supporting Information (SI) or as described previously,[21,28] isolated from marine sponges[38] or purchased [pyrrole (**24**), ethyl-4-bromopyrrole-2-carboxylate (**27**) and 2,3-dibromo-N-methylmaleimide (**28**)] from SigmaAldrich (St. Louis, MO). Names and structures for the compounds tested are summarized in Table SI1. All the HOCs were dissolved in dry DMSO (10 mM) and stored at −80 °C. Phenylmethylsulfonyl fluoride (PMSF), leupeptin hydrochloride, Mg-ATP, phosphocreatine, creatine phosphokinase, phosphoenolpyruvate, pyruvate kinase/lactic dehydrogenase, Na_2ATP, NADH were purchased from Sigma-Aldrich. Arsenazo III was purchased from Santa Cruz Biotechnology (Dallas, TE). Ryanodine was purchased from Ascent Scientific (Cambridge, MA) and dissolved in 100% ethanol and stored at 4 °C until use. [^{3}H]Ryanodine (specific activity: 56.6 Ci/ mmol) was obtained from PerkinElmer (Santa Clara, CA).

RyR1-Enriched Microsomal Preparations.

Microsomal membranes enriched in RyR1 and SERCA1a from the junctional region (JSR) were isolated from fast-twitch skeletal muscles of 1 year old male (2−2.5 kg) New Zealand White rabbits as detailed in SI and previously described.[39] Two independent microsomal preparations were used to conduct and replicate all assays. Protein concentrations were measured with the BCA protocol (Fisher, Waltham, MA).

Equilibrium [^{3}H]Ry Binding Analysis.

[^{3}H]Ry (56.6 Ci/ mmole) binding analysis was performed as previously described.[40] Briefly, 50 μg protein and 1 nM [^{3}H]Ry were utilized in the presence of vehicle or 0.05−20 μM of each HOC, and incubated with 500 μL of binding buffer at 37 °C for 3 h as described in detail in SI. At least 2 independent experiments were conducted for each [^{3}H]Ry binding analysis, each performed in triplicate or quintuplicate.

Measurements of SERCA1a Activity.

Activity of JSR Ca^{2+} ATPase was measured using a coupled enzyme assay monitoring the oxidation rate of NADH at 340 nm as described in SI and previous publication.[41] Thapsigargin (TG), a specific blocker of SERCA, was used as a control to discriminate between SERCA-dependent ATPase and nonspecific ATPase (TG-insensitive) activities. At least two independent preparations were utilized to test each compound in triplicate.

Measurements of Microsomal Ca^{2+} Fluxes and Ca^{2+} -Induced Ca^{2+} Release.

The measurements of Ca^{2+} uptake and release from microsomal membrane vesicles were performed by monitoring absorbance using metallochromic Ca^{2+} dye Arsenazo III at 650−700 nm at 35 °C as detailed in SI, and similar to previous methods described with metallochromic Ca^{2+} dye Antipyrylazo III.[42] Two different preparations were used for testing each compound in triplicate.

Data Analysis and Statistics.

Graphing and statistical analyses were performed using GraphPad Prism software (version 7.0; GraphPad Software Inc., San Diego, CA). Potency and efficacy values were determined by nonlinear regression with three-parameter equation and Bell-shaped equation. Statistical analysis of comparisons between the means of each group and means across all other groups, One-way ANOVA followed by post hoc Tukey's test was used. For comparisons made between mean of each test compound and the mean of the control, Dunnett's *post hoc* test was used to analyze the data at 95% confidence intervals.

RESULTS AND DISCUSSION

Structure−Activity Relationship for Marine HOCs toward RyR1.

The binding of Ry to multiple sites within the ion conduction pathway of RyRs results in complex influences on its channel gating behavior, stabilizing the open states at low (nM) and fully blocking the channel at higher (μM) concentrations.[39,43,44] Low nanomolar levels Ry binds preferentially to high-affinity sites only accessible when RyR channels are in the open state thus promoting SR/ER Ca^{2+} efflux (Ca^{2+} leak), which can have dramatic pathophysiological consequences.[45,46] Because of these properties, [^{3}H]Ry binding analysis has been broadly used to identify ligands that interact with RyRs and understand their structure−function relationships, and serves as a rapid throughput screening tool. Of 34 HOCs initially tested (Table SI1), 10 halogenated pyrroles, bipyrroles, indoles, maleimides and diphenylethers (**6, 13, 14, 17, 18, 19, 25, 28, 31,** and **34**) were identified to enhance [^{3}H]Ry binding to RyR1 ≥ 1.5-fold at 2 μM when compared to baseline (binding measured

in the presence of Veh alone, $p < 0.05$ vs Veh, Figure 1). These and an additional 4 HOCs (**15, 24, 26,** and **27**) were selected for further study based on their structural similarities to establish an initial structure activity relationship (SAR) using [^{3}H]Ry, Ca^{2+} ATPase, and Ca^{2+} flux measurements. On the basis of structural homologies, these compounds were classified into two major categories: (A) halogenated pyrroles, bipyrroles, maleimides, and indoles and (B) PBDE derivatives, as shown in Figure 2.

Active HOCs within group A enhanced the binding of [^{3}H]Ry to RyR1 in a concentration-dependent manner and their relative efficacies at 10 μM ranked **14** > **31** > **13** = **34**, whereas **24**, **26**, and **27** were inactive (Figure 3A, B).Interestingly **6** (2,3-dibromomaleimide), a naturally produced marine HOC, showed highly potent biphasic influences on RyR1, stabilizing the open state of RyR1 with an EC_{50} of 0.36 μM, and inhibiting with an IC_{50} of 3.0 μM (Figure 3A, C; table insert). Compound **6** was shown to form Michael adducts with protein Cys[47] and, therefore, raised the question whether its biphasic actions results from forming covalent adducts to hyper-reactive RyR1 Cys residues previously identified to confer redox-sensing properties and regulation to the RyR1 complex.[48–52] To better define the possible role of Cys-adducts in the biphasic response observed with **6**, the concentrationeffect relationship was extended to **31** and **34**, which are unable to form Cys-adducts, and commercially available 2, 3-dibromo-N-methylmaleimide (**28**) was also tested. Indeed, all three compounds produced biphasic modulation of RyR1 (Figure 3C), indicating that Michael addition to one or more reactive Cys was not required for the biphasic response. This conclusion was further supported by previous data indicating that 4′hydroxy-2,2′,4,5′-tetrabromodiphenyl ether (4-OH-BDE-49), also incapable of forming Michael adducts also exhibits biphasic actions toward RyR1, whereas BDE-49 activated in a monotonic manner.[53] Thus, biphasic activity was unlikely to be mediated by Cys modifications on RyR1, but more likely mediated by interaction with multiple binding sites on the homotetramer. 6-OH N-methylation of **6** decreased the apparent activation potency by 1.7-fold ($p < 0.05$) without altering inhibitory potency or maximum efficacy (Figure 3C, table insert). By comparison, **31** and **34** were 68- and 107-fold ($p < 0.01$) less potent activators, respectively, although they attained 2.5-fold higher maximum efficacy at 50 μM compared to that reached by **6** at 1 μM. Likewise **31** and **34** were weaker inhibitors than **6** (Figure 3C, table insert). Thus, not only is polybromination of the pyrrole essential for RyR1 activity, but also the 5-Br appeared to be especially important for optimizing activity. Hexabromobipyrrole is less active suggesting steric factors were important. Finally, we tested 2,3-dibromoindole (**14**) and its synthetic chlorinated analog 2,3-dichloroindole (**13**), and found that **14** is more active, indicating steric bulk and/or electron withdrawal from the indole ring were important for conferring activity toward RyR1.

A previous structure−activity study of anthropogenic PBDEs and OH-derivatives indicated that two *ortho*-Br substitutions were necessary for activating RyRs and that *meta*-Br further enhanced, whereas para-Br reduced, activity.[53] Of 13 naturally occurring PBDE derivatives identified in the marine environment and tested in the current study (Table SI1), only three were found to meet our criteria for efficacy toward RyR1 (i.e., significant enhancement of specific [^{3}H]Ry binding at 2 μM, $p < 0.05$ vs 1% vehicle control (Figures 1 and 2, group B). Consistent with previous findings, compounds **18** and **19** have at least two ortho-Br

substitutions with ranked efficacies at 10 μM of **18** > **19** (Figure 4). The importance of *para*-substituents was further underscored by the observation that *para*-OH is more active than *para*-methoxy (**18** vs **19**). With an additional *ortho*-hydroxy or ortho-methoxy, however, the 10 PBDE derivatives with a single *ortho*-Br that were tested, all failed to meet criteria for activity toward RyR1 (Table SI1 and Figure 1). Consistent with ortho-chlorination of NDL-PCBs,[40,53,54] monoortho-Br was generally less active than di-Br, although *meta* and *para* substitutions dictated the level of RyR1 activity. For example, *para*-methoxy, (**17**) was more active toward RyR1 than **15** with *para*-OH, further extending the structure−activity relationship for biosynthetic PBDEs.

Collectively, these data identified for the first time that halogenated pyrroles, bipyrroles and indoles of marine origin were modulators of RyR1 and have a stringent structural requirement that dictated their potency and efficacy. It is interesting to note that the pyrrole moiety at 2-position of ryanodine was essential for not only conferring high-affinity binding to mammalian RyR1, but was also shown essential for conferring toxicity to mice,[44,55] suggesting that the HOCs identified here may represent reduced structures sufficient to occupy the essential pyrrole docking site(s) and confer the biphasic actions of ryanodine on multiple high- and low-affinity binding sites on the RyR1 homotetrameric complex.[45,56–58]

Structure−Activity Relationship for Marine HOCs toward SERCA1a.

The efflux rate and amount of SR/ER Ca^{2+} released not only depends on the density and activities of RyR1 and IP_3R channels, but also is determined by the activity of ATP-dependent driven SERCA pumps necessary for reaccumulation of luminal Ca^{2+} and setting the ionic driving force that shapes Ca^{2+} transient properties. We therefore determined whether HOCs active toward RyR1 also influenced the activity of SERCA1a found in the same SR/ER membrane preparation tested for RyR1 activity.

Over 90% of the Ca^{2+}-dependent ATPase activity measured in the microsomal preparations could be attributed to SERCA1a in that it was inhibited by TG (Figure 5). These studies were focused principally on the HOCs in Group A but also compared **18** in Group B. Compounds **18** and **25** were identified as the most potent inhibitors of SERCA1a activity with >80% inhibition at 2.0 μM (Figure 5D and F), and ~90% inhibition at 10 μM (Figure 7). At 10 μM compounds **31, 14, 6**, and **34** showed intermediate SERCA1a inhibition (80, 60, 50, and 48%, respectively) (Figures 5B, 5E, SI1, and 5C), whereas **24, 26** and **27**, which were inactive toward RyR1, were also inactive toward SERCA1a (Figure 5G).

The degree and distribution of pyrrole bromination was an important factor for both RyR1 and SERCA1a activities, with **31** (tetrabromination) being most active, **34** being intermediate (2,3,5-bromination), and **26** (2, 3, 4-bromination) being inactive in both assays. These data indicate di-*ortho*-bromine substitution is an important contributor for both RyR1 and SERCA1a activity. This also extended to compound **25** (hexabromobipyrroles) that has two ortho-bromine substituents and possesses similar RyR1 activity as compound **34** (Figure 1). Compound **25** also exhibited the strongest SERCA inhibition (Figure 5D). As shown in the Figure SI3, compound **25** diminished the loading capacity of calcium into the

microsomal vesicles in a concentration-dependent manner, an effect compounded by targeting both RyR1 activation and SERCA1a inhibition.

Interestingly, 0.6−1.0 μM compound **6**, a dibromomaleimide maximally activated RyR1 (Figure 3) without inhibition of SERCA1a (Figure SI 1). In fact, the RyR1 inhibitory phase of **6** was detected at <5 μM, whereas SERCA1a inhibition was detected only at the highest concentration tested (10 μM) (Figure SI1).

Impact of RyR1 and SERCA1a Activities on Microsomal Ca^{2+} Dynamics.

The net uptake and release of Ca^{2+} across the SR/ER (microsomal) membrane compartments has been shown to depend on three principal factors: (1) activity of ATP-dependent SERCA pumps sequestering free cytoplasmic Ca^{2+} to a resting level of ~100 nM; (2) active release of luminal Ca^{2+} through mechanisms regulating RyRs and IP^3Rs channel activities; and (3) passive Ca^{2+} leakage out of the microsomal compartment through mechanisms that remain unclear, but are likely to involve distinct leaks states of RyRs and IP^3R, although additional mechanisms have been proposed.[59,60] We therefore set out to further evaluate how 9 HOCs that showed distinct patterns of RyR1 and SERCA1a activities influenced net Ca^{2+} flux across microsomal membranes (JSR) (Figure 6 and Figure SI2). Figure 6A depicts the Ca^{2+} transport assay that utilized the membrane-impermeant indicator Arsenazo III to record extra-vesicular Ca^{2+} in real-time. Flux of Ca^{2+} into (net uptake) or out of (net release) the vesicles depends on all three aforementioned factors. We therefore proceeded to test nine HOCs for their ability to trigger the release of Ca^{2+} accumulated after bolus addition of 4 × 45 nmole Ca^{2+} was completed during the loading phase of the experiment (Figure 6A, B). Since the Ca^{2+} driving force (i.e., the amount of Ca^{2+} loaded into the lumen of the vesicles) was kept consistent across experiments, the rates of release induced by HOCs could be directly compared.

Results of the analyzed initial release rates from these flux experiments generally followed predictions from the relative activities of HOCs toward RyR1 and SERCA1a (Figure 6C-G). Specifically, compounds **24, 26,** and **27** failed to trigger net release of accumulated Ca^{2+} from the microsomal vesicles (Figure 6H), consistent with their lack of activity toward both biochemical targets. By contrast, active HOCs triggered dose-dependent Ca^{2+} efflux with a rank order of **31** > **18** > **34** > **25** > **14**. The initial rates of Ca^{2+} efflux triggered by these HOCs followed their respective activities toward RyR1 and SERCA1a with the exception of the dibrominated indole **14** whose activity was significantly under-predicted by the Ca^{2+} flux rates it produced at either 5 or 10 μM, concentrations anticipated to largely stabilize a RyR1 open channel state while inhibiting SERCA1a ~55% (Figure 7). The discrepancy with compound **14** could be explained if an extended amount of time is needed to fully manifest stabilization of the open channel state, which is afforded by the 3-h incubation in [^{3}H]Ry binding assays but not the Ca^{2+} assay. Moreover, compound **14** may also inhibit RyR1 leak-states, which if blocked, can dramatically increase the Ca^{2+} loading capacity of the microsomal vesicles. Brominated macrocyclic bastadins isolated from the marine sponge *Ianthella basta*[61–66] and anthropogenic PCBs[16] have been previously shown to influence the balance of channel and leak states of RyR1, although whether this mechanism explains the results obtained with compound **14** remains to be determined.

Considering the potent biphasic activity of compound 6 on RyR1 (Figure 3) and its modest inhibitory activity toward SERCA1a (Figure SI1), it was not unexpected that high concentrations (5 and 10 μM), concentrations expected to completely inhibit RyR1 channels, failed to trigger net Ca^{2+} efflux added to Ca^{2+}-loaded microsomal vesicles (when the extravesicular free Ca^{2+} is very low; ~100 nM) (Figure SI2). However, an additional a large bolus (90 nmol) of Ca^{2+} to trigger Ca^{2+}-induced Ca^{2+}-release resulted in significantly higher rates of release than control (** $p < 0.01$, Figure SI2A and B). The sensitizing influences on calcium-induced calcium release (CICR) were observed in the presence of nanomolar 6 that should partially activate RyR1 without any SERCA1a inhibition, although their magnitude did not reach statistical significance (Figure SI2C and D).

The present results are significant because they identify several prominent naturally synthesized marine HOCs that directly target two major proteins whose functions work in opposition to tightly regulate net ER/SR Ca^{2+} dynamics, and thus, are essential for shaping localized and global Ca^{2+} signals that regulate a plethora of cellular functions.[16,67] From the perspective of chemical ecology, tetrabromopyrrole (**31**) has been recently isolated from *Pseudoalteromonas* bacteria and shown to serve specific habitat cues for the attachment and metamorphosis of benthic marine invertebrates, including coral *Acropora millepora* larvae and multiple Caribbean corals (*Orbicella franks*i and *Acropora palmata*) that settle onto crustose coralline algae.[29,30,68] The current findings may have widespread implications since motility, secretion and metamorphosis of planula are associated with the creation of crystalline substratum calcification mediated by precise Ca^{2+} signals.[29] HOCs, including *tetrabromopyrrole* and hexabromobipyrroles, extracted from *Pseudoalteromonas* bacteria that often associate with coralline algae-associated bacterium and *Chromobacterium* were reported to possess a spectrum of antibiotic, antifungal, antiprotozoal, antipathogen and antineoplastic activities.[69–73] Recently, natural sources of HOCs were shown to accumulate in marine organisms, especially apex predators such as seabirds and dolphins.[74–77]

A second, equally significant implication is the recent detection of several halopyrroles in DBPs, including compounds **31** and **34**, found in waste and drinking water treatment streams are cytotoxic, genotoxic and carcinogenic to mammalian cells.[31,32,34] The newly identified targets reported here and their neuroactive properties reported in the following paper (in preparation) provide important mechanistic clues about their potential disruptive influences on marine ecology and contributions to human health risks, especially given recent evidence that HOCs of biosynthetic and anthropogenic origins accumulate in marine mammals and human breast milk.24,27,74,75,77,78

Supplementary Material

Refer to Web version on PubMed Central for supplementary material.

■ ACKNOWLEDGMENTS

Supported by the National Institute of Environmental Health Sciences (R01 ES014901, P01 ES011269, P42 ES04699, P01 ES021921), US Environmental Protection Agency (STARR829388 and R833292), the National Science Foundation (OCE-1313747), the Natural Sciences and Engineering Research Council of Canada (NSERC-PDF to S.M.K.M.), the National Institutes of Health (R00ES026620 to V. A.), and China Scholarship Council (CSC 201507060027).

REFERENCES

(1). Agarwal V; El Gamal AA; Yamanaka K; Poth D; Kersten RD; Schorn M; Allen EE; Moore BS Biosynthesis of polybrominated aromatic organic compounds by marine bacteria. *Nat. Chem. Biol.* 2014, 10 (8), 640–7. [PubMed: 24974229]

(2). Gribble GW *Naturally Occurring Organohalogen Compounds*: A Comprehensive Update; Springer-Verlag: Wien, Austria, 2010; p xv, 613 p.

(3). Lyche JL; Rosseland C; Berge G; Polder A Human health risk associated with brominated flame-retardants (BFRs). *Environ. Int.* 2015, 74, 170–80. [PubMed: 25454234]

(4). Beyer A; Biziuk M Environmental fate and global distribution of polychlorinated biphenyls. Rev. Environ. *Contam. Toxicol.* 2009, 201, 137–58. [PubMed: 19484591]

(5). Nicklisch SCT; Bonito LT; Sandin S; Hamdoun A Geographic Differences in Persistent Organic Pollutant Levels of Yellowfin Tuna. *Environ. Health Perspect.* 2017, 125 (6), 067014. [PubMed: 28686554]

(6). Marek RF; Thorne PS; Herkert NJ; Awad AM; Hornbuckle KC Airborne PCBs and OH-PCBs Inside and Outside Urban and Rural US Schools. *Environ. Sci. Technol.* 2017, 51 (14), 7853–7860. [PubMed: 28656752]

(7). Martinez A; Hadnott BN; Awad AM; Herkert NJ; Tomsho K; Basra K; Scammell MK; Heiger-Bernays W; Hornbuckle KC Release of Airborne Polychlorinated Biphenyls from New Bedford Harbor Results in Elevated Concentrations in the Surrounding Air. Environ. Sci. Technol. *Lett.* 2017, 4 (4), 127–131.

(8). Abbasi NA; Malik RN; Frantz A; Jaspers VL A review on current knowledge and future prospects of organohalogen contaminants (OHCs) in Asian birds. Sci. Total Environ 2016, 542, 411–426. [PubMed: 26520266]

(9). Letcher RJ; Bustnes JO; Dietz R; Jenssen BM; Jorgensen EH; Sonne C; Verreault J; Vijayan MM; Gabrielsen GW Exposure and effects assessment of persistent organohalogen contaminants in arctic wildlife and fish. *Sci. Total Environ.* 2010, 408 (15), 2995–3043. [PubMed: 19910021]

(10). Koh WX; Hornbuckle KC; Wang K; Thorne PS Serum polychlorinated biphenyls and their hydroxylated metabolites are associated with demographic and behavioral factors in children and mothers. *Environ. Int.* 2016, 94, 538–545. [PubMed: 27352881]

(11). Safe S; Hutzinger O Polychlorinated biphenyls (PCBs) and polybrominated biphenyls (PBBs): biochemistry, toxicology, and mechanism of action. Crit Rev. Toxicol 1984, 13 (4), 319–395. [PubMed: 6091997]

(12). Johnson-Restrepo B; Kannan K; Rapaport DP; Rodan BD Polybrominated diphenyl ethers and polychlorinated biphenyls in human adipose tissue from New York. *Environ. Sci. Technol.* 2005, 39 (14), 5177–82. [PubMed: 16082945]

(13). Johnson-Restrepo B; Kannan K; Addink R; Adams DH Polybrominated diphenyl ethers and polychlorinated biphenyls in a marine foodweb of coastal Florida. *Environ. Sci. Technol.* 2005, 39 (21), 8243–50. [PubMed: 16294860]

(14). Berghuis SA; Bos AF; Sauer PJ; Roze E Developmental neurotoxicity of persistent organic pollutants: an update on childhood outcome. *Arch. Toxicol.* 2015, 89 (5), 687–709. [PubMed: 25618547]

(15). Stamou M; Streifel KM; Goines PE; Lein PJ Neuronal connectivity as a convergent target of gene x environment interactions that confer risk for Autism Spectrum Disorders. *Neurotoxicol. Teratol.* 2013, 36, 3–16. [PubMed: 23269408]

(16). Pessah IN; Cherednichenko G; Lein PJ Minding the calcium store: Ryanodine receptor activation as a convergent mechanism of PCB toxicity. *Pharmacol. Ther.* 2010, 125 (2), 260–85. [PubMed: 19931307]

(17). Costa LG; Giordano G Developmental neurotoxicity of polybrominated diphenyl ether (PBDE) flame retardants. Neuro-Toxicology 2007, 28 (6), 1047–1067.

(18). Vaillancourt FH; Yeh E; Vosburg DA; Garneau-Tsodikova S; Walsh CT Nature's inventory of halogenation catalysts: Oxidative strategies predominate. *Chem. Rev.* 2006, 106 (8), 3364–3378. [PubMed: 16895332]

(19). Agarwal V; Blanton JM; Podell S; Taton A; Schorn MA; Busch J; Lin Z; Schmidt EW; Jensen PR; Paul VJ; Biggs JS; Golden JW; Allen EE; Moore BS Metagenomic discovery of polybrominated diphenyl ether biosynthesis by marine sponges. *Nat. Chem. Biol.* 2017, 13 (5), 537–543. [PubMed: 28319100]

(20). Agarwal V; Miles ZD; Winter JM; Eustaquio AS; El Gamal AA; Moore BS Enzymatic Halogenation and Dehalogenation Reactions: Pervasive and Mechanistically Diverse. *Chem. Rev.* 2017, 117, 5619. [PubMed: 28106994]

(21). El Gamal A; Agarwal V; Rahman I; Moore BS Enzymatic Reductive Dehalogenation Controls the Biosynthesis of Marine Bacterial Pyrroles. *J. Am. Chem. Soc.* 2016, 138 (40), 13167–13170. [PubMed: 27676265]

(22). Teuten EL; Xu L; Reddy CM Two abundant bioaccumulated halogenated compounds are natural products. Science 2005, 307 (5711), 917–920. [PubMed: 15705850]

(23). Hoh E; Dodder NG; Lehotay SJ; Pangallo KC; Reddy CM; Maruya KA Nontargeted comprehensive two-dimensional gas chromatography/time-of-flight mass spectrometry method and software for inventorying persistent and bioaccumulative contaminants in marine environments. *Environ. Sci. Technol.* 2012, 46 (15), 8001–8. [PubMed: 22712571]

(24). Tittlemier SA; Simon M; Jarman WM; Elliott JE; Norstrom RJ Identification of a novel $C_{10}H_6N_2Br_4Cl_2$ heterocyclic compound in seabird eggs. A bioaccumulating marine natural product? *Environ. Sci. Technol.* 1999, 33 (1), 26–33.

(25). Pangallo K; Nelson RK; Teuten EL; Pedler BE; Reddy CM Expanding the range of halogenated 1′-methyl-1,2′-bipyrroles (MBPs) using GC/ECNI-MS and GCxGC/TOF-MS. Chemosphere 2008, 71 (8), 1557–65. [PubMed: 18191175]

(26). Reddy CM; Xu L; O'Neil GW; Nelson RK; Eglinton TI; Faulkner DJ; Norstrom R; Ross PS; Tittlemier SA Radiocarbon evidence for a naturally produced, bioaccumulating halogenated organic compound. *Environ. Sci. Technol.* 2004, 38 (7), 1992–7. [PubMed: 15112798]

(27). Vetter W; Alder L; Kallenborn R; Schlabach M Determination of Q1, an unknown organochlorine contaminant, in human milk, Antarctic air, and further environmental samples. *Environ. Pollut.* 2000, 110 (3), 401–9. [PubMed: 15092819]

(28). El Gamal A; Agarwal V; Diethelm S; Rahman I; Schorn MA; Sneed JM; Louie GV; Whalen KE; Mincer TJ; Noel JP; Paul VJ; Moore BS Biosynthesis of coral settlement cue tetrabromopyrrole in marine bacteria by a uniquely adapted brominase-thioesterase enzyme pair. Proc. *Natl. Acad. Sci. U. S. A.* 2016, 113 (14), 3797–802. [PubMed: 27001835]

(29). Sneed JM; Sharp KH; Ritchie KB; Paul VJ The chemical cue tetrabromopyrrole from a biofilm bacterium induces settlement of multiple Caribbean corals. Proc. R. Soc. London, Ser. B 2014, 281 (1786), 20133086.

(30). Tebben J; Tapiolas DM; Motti CA; Abrego D; Negri AP; Blackall LL; Steinberg PD; Harder T Induction of larval metamorphosis of the coral *Acropora millepora* by tetrabromopyrrole isolated from a *Pseudoalteromonas* bacterium. PLoS One 2011, 6 (4), e19082. [PubMed: 21559509]

(31). Richardson SD; Thruston AD; Rav-Acha C; Groisman L; Popilevsky I; Juraev O; Glezer V; McKague AB; Plewa MJ; Wagner ED Tribromopyrrole, Brominated Acids, and Other Disinfection Byproducts Produced by Disinfection of Drinking Water Rich in Bromide. *Environ. Sci. Technol.* 2003, 37 (17), 3782–3793. [PubMed: 12967096]

(32). Richardson SD; Plewa MJ; Wagner ED; Schoeny R; Demarini DM Occurrence, genotoxicity, and carcinogenicity of regulated and emerging disinfection by-products in drinking water: a review and roadmap for research. Mutat. Res, *Rev. Mutat. Res.* 2007, 636 (1−3), 178–242. [PubMed: 17980649]

(33). Plewa MJ; Wagner ED; Mitch WA Comparative Mammalian cell cytotoxicity of water concentrates from disinfected recreational pools. *Environ. Sci. Technol.* 2011, 45 (9), 4159–65. [PubMed: 21466188]

(34). Yang M; Zhang X Halopyrroles: A new group of highly toxic disinfection byproducts formed in chlorinated saline wastewater. Environ. Sci. Technol 2014, 48 (20), 11846–52. [PubMed: 25236171]

(35). Dong S; Lu J; Plewa MJ; Nguyen TH Comparative Mammalian Cell Cytotoxicity of Wastewaters for Agricultural Reuse after Ozonation. Environ. *Sci. Technol*. 2016, 50 (21), 11752–11759. [PubMed: 27689387]

(36). Lanner JT; Georgiou DK; Joshi AD; Hamilton SL Ryanodine receptors: structure, expression, molecular details, and function in calcium release. Cold Spring Harbor Perspect. Biol 2010, 2 (11), a003996.

(37). Luciani DS; Gwiazda KS; Yang TLB; Kalynyak TB; Bychkivska Y; Frey MHZ; Jeffrey KD; Sampaio AV; Underhill TM; Johnson JD Roles of IP3R and RyR Ca^{2+} Channels in Endoplasmic Reticulum Stress and beta-Cell Death. Diabetes 2009, 58 (2), 422–432. [PubMed: 19033399]

(38). Agarwal V; Li J; Rahman I; Borgen M; Aluwihare LI; Biggs JS; Paul VJ; Moore BS Complexity of naturally produced polybrominated diphenyl ethers revealed via mass spectrometry. *Environ. Sci. Technol*. 2015, 49 (3), 1339–46. [PubMed: 25559102]

(39). Pessah IN; Francini AO; Scales DJ; Waterhouse AL; Casida JE Calcium−ryanodine receptor complex. Solubilization and partial characterization from skeletal muscle junctional sarcoplasmic reticulum vesicles. *J. Biol. Chem*. 1986, 261 (19), 8643–8648. [PubMed: 3722165]

(40). Pessah IN; Hansen LG; Albertson TE; Garner CE; Ta TA; Do Z; Kim KH; Wong PW Structure-activity relationship for noncoplanar polychlorinated biphenyl congeners toward the ryanodine receptor-Ca2+ channel complex type 1 (RyR1). *Chem. Res. Toxicol*. 2006, 19 (1), 92–101. [PubMed: 16411661]

(41). Feng W; Cherednichenko G; Ward CW; Padilla IT; Cabrales E; Lopez JR; Eltit JM; Allen PD; Pessah IN Green tea catechins are potent sensitizers of ryanodine receptor type 1 (RyR1). Biochem. Pharmacol. 2010, 80 (4), 512–21. [PubMed: 20471964]

(42). Wong PW; Pessah IN Ortho-substituted polychlorinated biphenyls alter calcium regulation by a ryanodine receptor-mediated mechanism: structural specificity toward skeletal- and cardiac-type microsomal calcium release channels. *Mol. Pharmacol*. 1996, 49 (4), 740–751. [PubMed: 8609904]

(43). Zimanyi I; Buck E; Abramson JJ; Mack MM; Pessah IN Ryanodine induces persistent inactivation of the Ca^{2+} release channel from skeletal muscle sarcoplasmic reticulum. *Mol. Pharmacol*. 1992, 42 (6), 1049–1057. [PubMed: 1480132]

(44). Waterhouse AL; Pessah IN; Francini AO; Casida JE Structural aspects of ryanodine action and selectivity. *J. Med. Chem*. 1987, 30 (4), 710–6. [PubMed: 2435905]

(45). Pessah IN; Zimanyi I Characterization of multiple [3H]ryanodine binding sites on the Ca^{2+} release channel of sarcoplasmic reticulum from skeletal and cardiac muscle: Evidence for a sequential mechanism in ryanodine action. *Mol. Pharmacol*. 1991, 39 (5), 679–689. [PubMed: 1851961]

(46). Zucchi R; RoncaTestoni S The sarcoplasmic reticulum Ca^{2+} channel/ryanodine receptor: Modulation by endogenous effectors, drugs and disease states. *Pharmacol. Rev*. 1997, 49 (1), 1–51. [PubMed: 9085308]

(47). Morgan RE; Chudasama V; Moody P; Smith MEB; Caddick S A novel synthetic chemistry approach to linkage-specific ubiquitin conjugation. *Org. Biomol. Chem*. 2015, 13 (14), 4165–4168. [PubMed: 25736233]

(48). Phimister AJ; Lango J; Lee EH; Ernst-Russell MA; Takeshima H; Ma J; Allen PD; Pessah IN Conformationdependent stability of junctophilin 1 (JP1) and ryanodine receptor type 1 (RyR1) channel complex is mediated by their hyper-reactive thiols. *J. Biol. Chem*. 2007, 282 (12), 8667–77. [PubMed: 17237236]

(49). Aracena-Parks P; Goonasekera SA; Gilman CP; Dirksen RT; Hidalgo C; Hamilton SL Identification of cysteines involved in S-nitrosylation, S-glutathionylation, and oxidation to disulfides in ryanodine receptor type 1. *J. Biol. Chem*. 2006, 281 (52), 40354–68. [PubMed: 17071618]

(50). Voss AA; Lango J; Ernst-Russell M; Morin D; Pessah IN Identification of hyperreactive cysteines within ryanodine receptor type 1 by mass spectrometry. *J. Biol. Chem*. 2004, 279 (33), 34514–34520. [PubMed: 15197184]

(51). Pessah IN; Kim KH; Feng W Redox sensing properties of the ryanodine receptor complex. *Front. Biosci., Landmark Ed*. 2002, 7, a72–a79.

(52). Feng W; Liu G; Allen PD; Pessah IN Transmembrane redox sensor of ryanodine receptor complex. *J. Biol. Chem*. 2000, 275 (46), 35902–7. [PubMed: 10998414]

(53). Kim KH; Bose DD; Ghogha A; Riehl J; Zhang R; Barnhart CD; Lein PJ; Pessah IN Para- and ortho-substitutions are key determinants of polybrominated diphenyl ether activity toward ryanodine receptors and neurotoxicity. Environ. Health Perspect 2011, 119 (4), 519–526. [PubMed: 21106467]

(54). Holland EB; Feng W; Zheng J; Dong Y; Li X; Lehmler HJ; Pessah IN An Extended Structure-Activity Relationship of Nondioxin-Like PCBs Evaluates and Supports Modeling Predictions and Identifies Picomolar Potency of PCB 202 Towards Ryanodine Receptors. Toxicol. Sci 2017, 155 (1), 170–181. [PubMed: 27655348]

(55). Welch W; Sutko JL; Mitchell KE; Airey J; Ruest L The pyrrole locus is the major orienting factor in ryanodine binding. Biochemistry 1996, 35 (22), 7165–7173. [PubMed: 8679544]

(56). Meissner G The structural basis of ryanodine receptor ion channel function. *J. Gen. Physiol*. 2017, 149 (12), 1065–1089. [PubMed: 29122978]

(57). Zimanyi I; Buck E; Abramson JJ; Mack MM; Pessah IN Ryanodine Induces Persistent Inactivation of the Ca^{2+} Release Channel from Skeletal-Muscle Sarcoplasmic-Reticulum. *Mol. Pharmacol*. 1992, 42 (6), 1049–1057. [PubMed: 1480132]

(58). Buck E; Zimanyi I; Abramson JJ; Pessah IN Ryanodine stabilizes multiple conformational states of the skeletal muscle calcium release channel. *J. Biol. Chem*. 1992, 267 (33), 23560–53567. [PubMed: 1331089]

(59). Popugaeva E; Pchitskaya E; Bezprozvanny I Dysregulation of neuronal calcium homeostasis in Alzheimer's disease - A therapeutic opportunity? *Biochem. Biophys. Res. Commun*. 2017, 483 (4), 998–1004. [PubMed: 27641664]

(60). Takeshima H; Venturi E; Sitsapesan R New and notable ionchannels in the sarcoplasmic/endoplasmic reticulum: do they support the process of intracellular Ca(2)(+) release? *J. Physiol*. 2015, 593 (15), 3241–51. [PubMed: 26228553]

(61). Masuno MN; Pessah IN; Olmstead MM; Molinski TF Simplified cyclic analogues of bastadin-5. Structure-activity relationships for modulation of the RyR1/FKBP12 Ca^{2+} channel complex. *J. Med. Chem*. 2006, 49 (15), 4497–511. [PubMed: 16854055]

(62). Gonzalez A; Kirsch WG; Shirokova N; Pizarro G; Brum G; Pessah IN; Stern MD; Cheng H; Rios E Involvement of multiple intracellular release channels in calcium sparks of skeletal muscle. *Proc. Natl. Acad. Sci. U. S. A*. 2000, 97 (8), 4380–5. [PubMed: 10759554]

(63). Chen L; Molinski TF; Pessah IN Bastadin 10 stabilizes the open conformation of the ryanodine-sensitive Ca(2+) channel in an FKBP12-dependent manner. *J. Biol. Chem*. 1999, 274 (46), 32603–12. [PubMed: 10551814]

(64). Pessah IN; Molinski TF; Meloy TD; Wong P; Buck ED; Allen PD; Mohr FC; Mack MM Bastadins relate ryanodinesensitive and -insensitive Ca^{2+} efflux pathways in skeletal SR and BC3H1 cells. *Am. J. Physiol*. 1997, 272 (2), C601–C614. [PubMed: 9124304]

(65). Franklin MA; Penn SG; Lebrilla CB; Lam TH; Pessah IN; Molinski TF Bastadin 20 and bastadin O-sulfate esters from Ianthella basta: novel modulators of the Ry1R FKBP12 receptor complex. *J. Nat. Prod*. 1996, 59 (12), 1121–7. [PubMed: 8988595]

(66). Mack MM; Molinski TF; Buck ED; Pessah IN Novel modulators of skeletal muscle FKBP12/calcium channel complex from Ianthella basta. Role of FKBP12 in channel gating. *J. Biol. Chem*. 1994, 269 (37), 23236−23249. [PubMed: 8083229]

(67). Berridge MJ Calcium microdomains: organization and function. Cell Calcium 2006, 40 (5−6), 405–12. [PubMed: 17030366]

(68). Rogers CL; Thomas MB Calcification in the planula and polyp of the hydroid Hydractinia symbiolongicarpus (Cnidaria, Hydrozoa). *J. Exp Biol*. 2001, 204, 2657–2666. [PubMed: 11533115]

(69). Burkholder PR; Pfister RM; Leitz FH Production of a Pyrrole Antibiotic by a Marine Bacterium. *Appl. Microbiol*. 1966, 14 (4), 649–653. [PubMed: 4380876]

(70). Andersen RJ; Wolfe MS; Faulkner DJ Autotoxic Antibiotic Production by a Marine Chromobacterium. *Mar. Biol*. 1974, 27, 281–285.

(71). Isnansetyo A; Kamei Y MC21-A, a Bactericidal Antibiotic Produced by a New Marine Bacterium, Pseudoalteromonas phenolica sp. nov. O-BC30T, against Methicillin-Resistant Staphylococcus aureus. Antimicrob. *Agents Chemother.* 2003, 47 (2), 480–488. [PubMed: 12543647]

(72). Tebben J; Motti C; Tapiolas D; Thomas-Hall P; Harder T A coralline algal-associated bacterium, pseudoalteromonas strain J010, yields five new korormicins and a bromopyrrole. Mar. Drugs 2014, 12 (5), 2802–15. [PubMed: 24828288]

(73). Xiong S; Pang HD; Fan J; Ge F; Yang XX; Liu QY; Liao XJ; Xu SH In vitro and in vivo antineoplastic activity of a novel bromopyrrole and its potential mechanism of action. Br. *J. Pharmacol.* 2010, 159 (4), 909–18. [PubMed: 20067467]

(74). Millow CJ; Mackintosh SA; Lewison RL; Dodder NG; Hoh E Identifying bioaccumulative halogenated organic compounds using a nontargeted analytical approach: seabirds as sentinels. PLoS One 2015, 10 (5), e0127205. [PubMed: 26020245]

(75). Shaul NJ; Dodder NG; Aluwihare LI; Mackintosh SA; Maruya KA; Chivers SJ; Danil K; Weller DW; Hoh E Nontargeted biomonitoring of halogenated organic compounds in two ecotypes of bottlenose dolphins (Tursiops truncatus) from the Southern California Bight. *Environ. Sci. Technol.* 2015, 49 (3), 1328–38. [PubMed: 25526519]

(76). Mackintosh SA; Dodder NG; Shaul NJ; Aluwihare LI; Maruya KA; Chivers SJ; Danil K; Weller DW; Hoh E Newly Identified DDT-Related Compounds Accumulating in Southern California Bottlenose Dolphins. *Environ. Sci. Technol.* 2016, 50 (22), 12129–12137. [PubMed: 27737539]

(77). Alonso MB; Maruya KA; Dodder NG; Lailson-Brito J, Jr.; Azevedo A; Santos-Neto E; Torres JP; Malm O; Hoh E Nontargeted Screening of Halogenated Organic Compounds in Bottlenose Dolphins (Tursiops truncatus) from Rio de Janeiro, Brazil. Environ. Sci. Technol 2017, 51 (3), 1176–1185. [PubMed: 28055195]

(78). Stapleton HM; Dodder NG; Kucklick JR; Reddy CM; Schantz MM; Becker PR; Gulland F; Porter BJ; Wise SA Determination of HBCD, PBDEs and MeO-BDEs in California sea lions (Zalophus californianus) stranded between 1993 and 2003. *Mar. Pollut. Bull.* 2006, 52 (5), 522−31. [PubMed: 16293266]

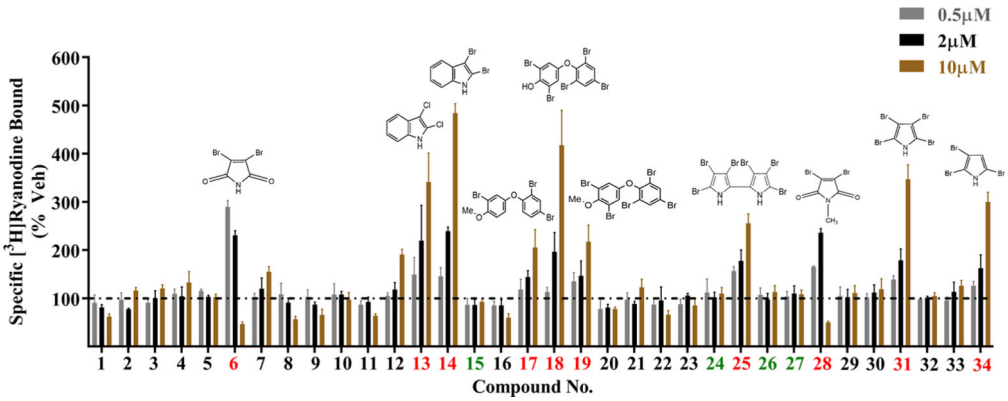

Figure 1.

Screening results of 34 organohalogens using [^{3}H]Ry binding analysis. Compounds in red color represent significant effects toward RyR1 were found at 2 μM at a threshold of $p <$ 0.05 compared with vehicle control using one-way ANOVA followed by Dunnett's multiple comparisons test. Compounds in green color were those inactive toward RyR1, and they are selected because of their structure properties. Data shown in the figure were conducted from 2 to 3 different preparations with triplicates for each preparation and were normalized to 1% DMSO control (% Veh) and expressed as mean ± SD Table SI1 summarizes the chemical structures tested.

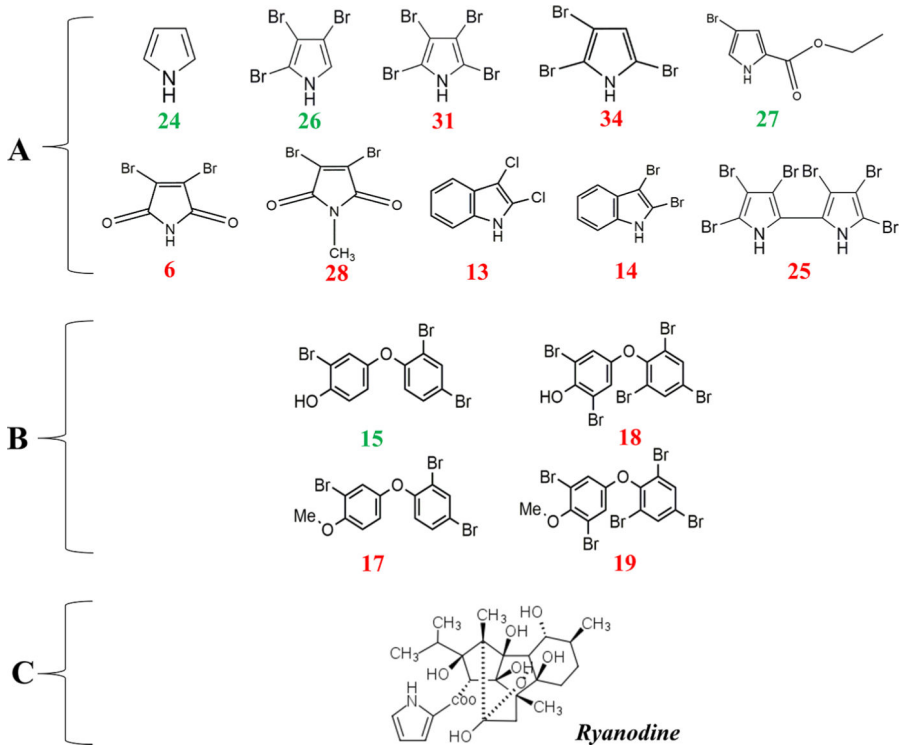

Figure 2.

Compounds selected for further evaluation for their activities toward RyR1, SERCA1a, and microsomal Ca^{2+} flux. (A) Structures of selected pyrroles, bipyrroles, maleimides and indoles. (B) Structures of PBDE derivatives of marine selected for further analysis in [^{3}H]Ry binding, SERCA1 activity and Ca^{2+} assays. (C) Structure of ryanodine.

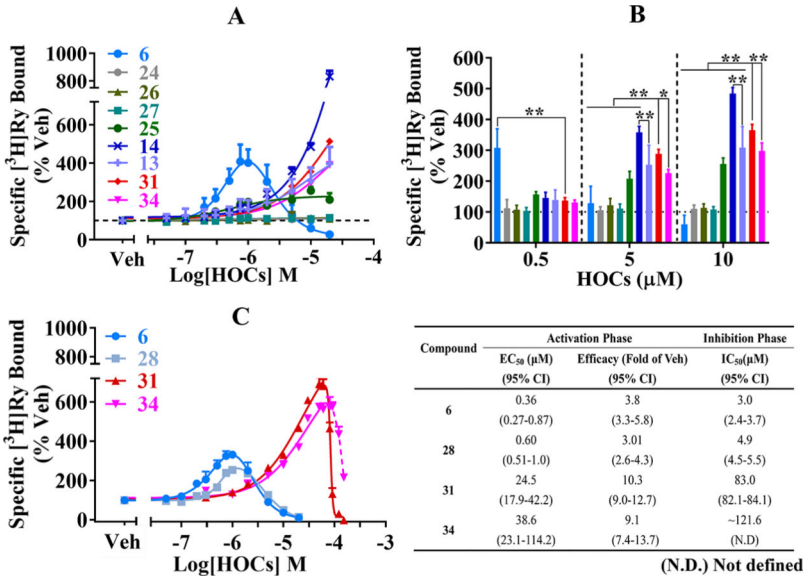

Compound	Activation Phase		Inhibition Phase
	EC_{50} (μM) (95% CI)	Efficacy (Fold of Veh) (95% CI)	IC_{50}(μM) (95% CI)
6	0.36 (0.27-0.87)	3.8 (3.3-5.8)	3.0 (2.4-3.7)
28	0.60 (0.51-1.0)	3.01 (2.6-4.3)	4.9 (4.5-5.5)
31	24.5 (17.9-42.2)	10.3 (9.0-12.7)	83.0 (82.1-84.1)
34	38.6 (23.1-114.2)	9.1 (7.4-13.7)	~121.6 (N.D)

(N.D.) Not defined

Figure 3.

Halogenated pyrroles, bipyrroles, maleimides and indoles exhibit stringent structure−activity relationship toward RyR1. Panel A shows concentration−response curves expressed as specifically bound [^{3}H]Ry to RyR1-enriched microsomal membranes (JSR) isolated as described in Materials and Methods. Data were fitted with three-parameter or Bell-shaped (compound **6**) nonlinear regression with Graph Pad 7.03. Panel B shows stimulation relative to vehicle (1% DMSO) control (% of Veh; dashed line). Panel C shows results from an expanded concentration range to quantify biphasic parameters fitted as described in panel A for compounds **6**, **28**, and **31**. The activation phase for **34** was fitted with a threeparameter equation but lacked sufficient data to fit the inhibition phase (dashed line). Parameters obtained from curve-fitting are summarized in inserted table. Data shown are from 2 to 3 independent preparations conducted in triplicates or quintuplicates and expressed as Mean ± SD. With Graph Pad 7.03, one-way ANOVA followed by Tukey's multiple comparisons test was used to determine the significance among specific compounds. * $p < 0.05$ and ** $p < 0.01$.

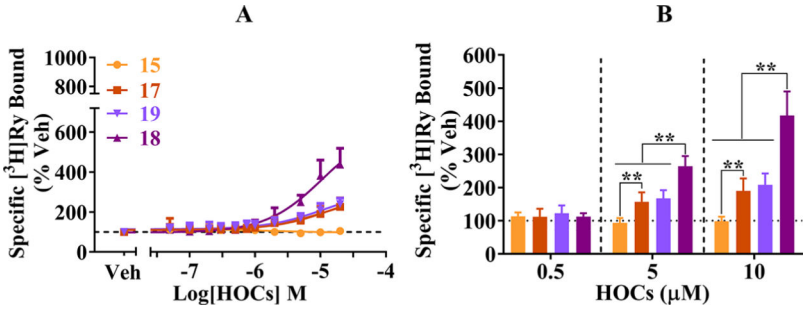

Figure 4.

Activity of PBDE derivatives of marine origin toward [^{3}H]Ry binding to RyR1. Panel A shows concentration−response curves for [^{3}H]Rybinding to RyR1-enriched microsomal membranes (JSR) expressed as % of vehicle (Veh) control (1% DMSO). Panel B shows relative binding levels obtained at 0.5, 5, and 10 μM of test compound. Each color corresponds to the specific compound identified in the key shown in panel A. The dashed line indicates baseline binding in the presence of Veh (i.e., 100%). Data shown are from 2 to 3 independent preparations conducted in triplicates or quintuplicates and expressed as mean ± SD. With Graph Pad 7.03, one-way ANOVA, followed by Tukey's multiple comparisons test was used to determine the significance among specific compounds. ** $p < 0.01$.

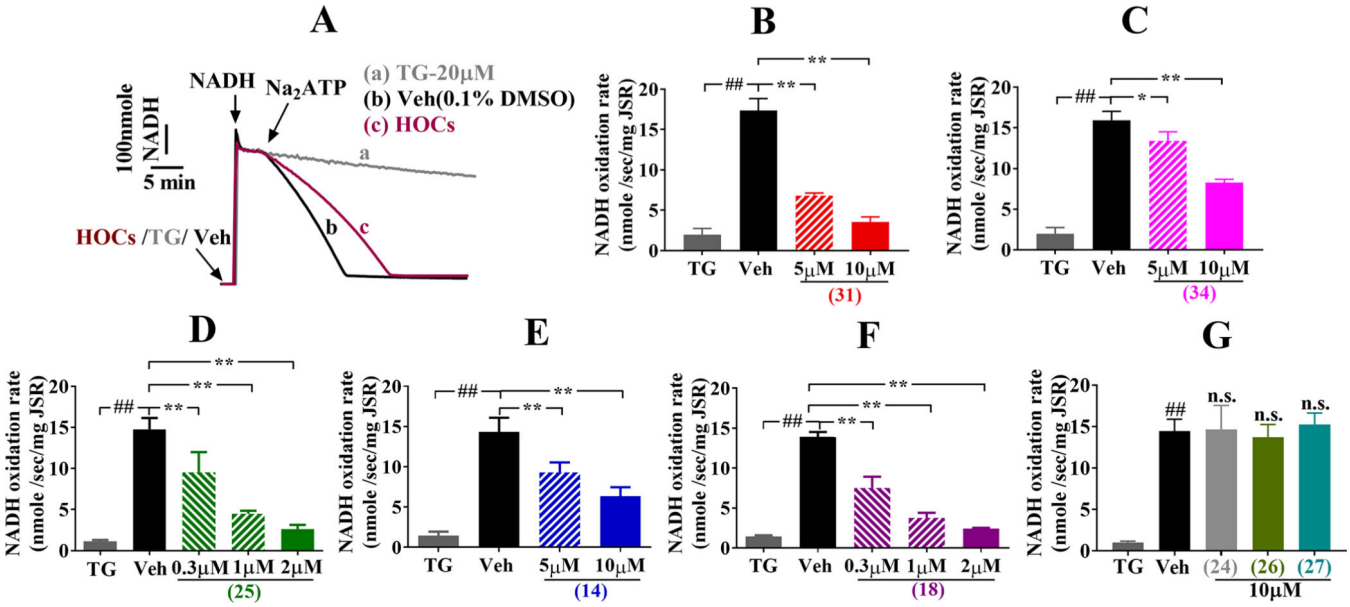

Figure 5.

Inhibition of TG-sensitive SERCA1a Ca^{2+} ATPase activity by selected HOCs of marine origin. (A) Representative traces showing the oxidation of NADH in the coupled enzyme assay was monitored by measuring absorbance at 340−400 nm. Veh (0.1% DMSO), TG (thapsigargin, 20 μM) or a HOC was added into separate reactions cuvettes before addition of NADH and Na_2ATP to initiate the reactions. The oxidation rate of NADH in the presence of TG, Veh or test compounds were summarized in bar graph (B−G). Two different microsomal (JSR) preparations were used to calculate the summary data for each group, and each performed in triplicates or quintuplicates. Data shown as Mean ± SD and statistical differences assessed by one-way ANOVA, followed by Dunnett's multiple comparisons test was performed using Graph Pad 7.03. * $p < 0.05$, ** $p < 0.01$ vs Veh, ## $p < 0.01$ vs TG, and n.s. indicates no significant compared with Veh.

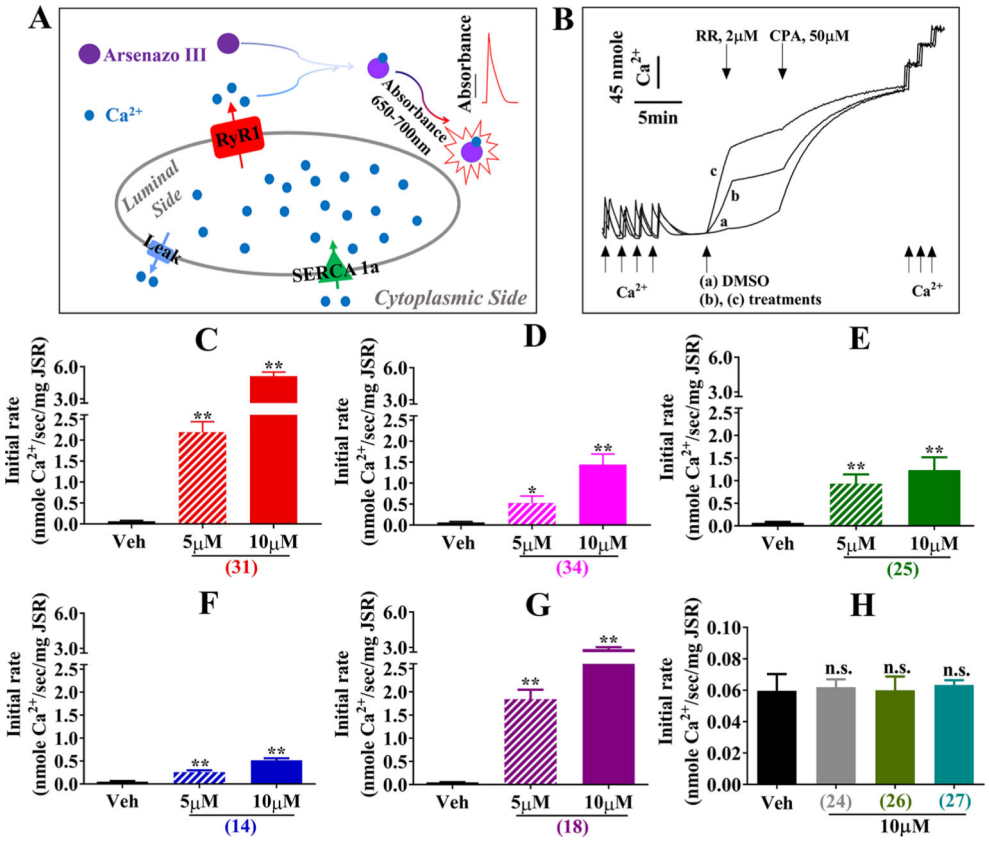

Figure 6.

Microsomal Ca^{2+} release triggered by selected HOCs of marine origin. (A) Schematic illustration showing the Ca^{2+} transport system monitored with Ca^{2+} dye Arsenozo III. (B) Representative traces of Ca^{2+} fluxes. Microsomal (JSR) vesicles were loaded with 4 sequential additions of 45 nmole $CaCl_2$, 60−90 s after the final bolus of Ca^{2+} was accumulated into vesicles, vehicle (0.2% DMSO, a) or test compounds (b or c) was introduced into one of the cuvettes. Ruthenium red (RR, 2 μM), a RyR blocker, was then added to each cuvettes to confirm the engagement of RyR1 followed by addition of SERCA inhibitor, cyclopiazonic acid (CPA, 50 μM), and $CaCl_2$ were added to calibrate absorbance unit into absolute Ca^{2+} in nmol. The Ca^{2+} release rate of initial 60 s upon the addition of Veh or test compounds (5 or 10 μM) are summarized in Panels C−H. Data shown are from 3 to 6 independent experiments using 2 different microsomal membrane preparations. Data expressed as Mean ± SD and one-way ANOVA followed by Dunnett's multiple comparisons test was performed using Graph Pad 7.03. *$p < 0.05$, **$p < 0.01$ vs Veh. And n.s. indicates no significant difference compared with Veh.

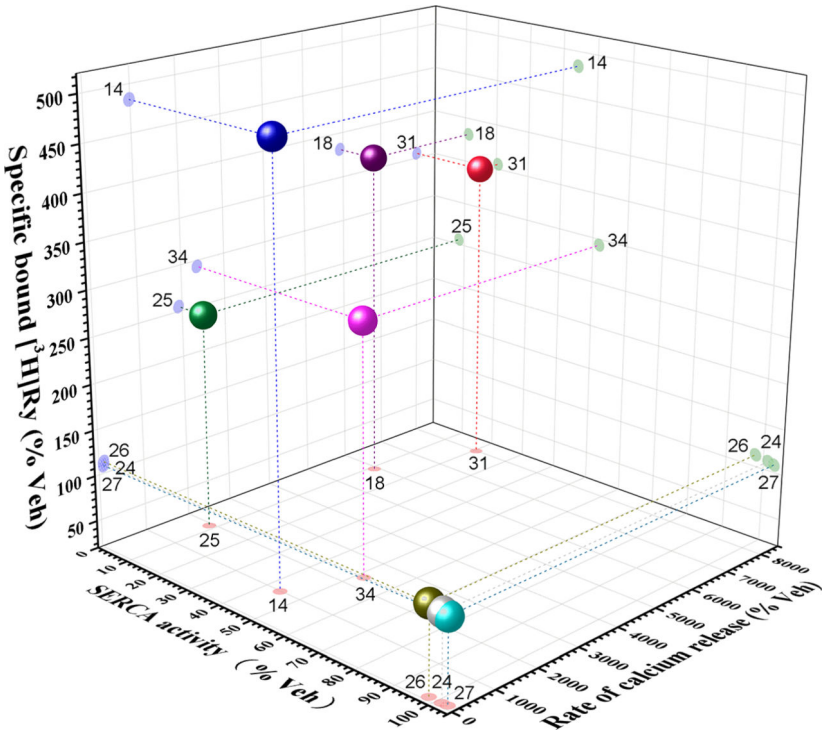

Figure 7.

3D trajectory plot showing the relationships among parameters calculated from [^{3}H]Ry-binding, SERCA1a activity and Ca^{2+} release rates from microsomal (JSR) membranes. Each individually colored sphere represents data extracted from one compound at 10 μM that are presented in the Figures 3–6. Veh indicates DMSO control. See text for further explanation.